

Article

On the Employment of a Chloride or Fluoride Salt Fuel System in Advanced Molten Salt Reactors, Part 1: Thermophysical Properties and Core Criticality

Omid Noori-kalkhoran ^{1,2,*}, Dzianis Litskevich ¹, Anna Detkina ¹, Lakshay Jain ¹, Gregory Cartland-Glover ³ and Bruno Merk ¹

¹ School of Engineering, The University of Liverpool, Liverpool L69 3GH, UK

² School of Engineering, Cardiff University, The Parade, Cardiff CF24 3AA, UK

³ Scientific Computing Department, Science and Technology Facilities Council, Daresbury Laboratory, SciTech Daresbury, Warrington WA4 4AD, UK

* Correspondence: o.noorikalkhoran@liverpool.ac.uk or noorikalkhorano@cardiff.ac.uk

Abstract: Molten salt reactors (MSRs), as one of the six main technologies of Gen IV, can meet the broad area of sustainability, economics, safety and reliability, proliferation resistance and physical protection goals. One of the main and first challenges in designing molten salt fast reactors (MSFRs) is the selection of an appropriate molten salt fuel system based on the envisaged applications and objectives. In this study's series, a full-scope evaluation has been conducted about employing either chloride or fluoride salt fuels as the main competitors' candidates for fuel salt in MSFR designs. Two distinguished projects, EVOL (CNRS, Grenoble-France), based on fluoride salt, and iMAGINE (The University of Liverpool, UK), based on chloride salts, were considered in order to achieve this goal as case studies. The first part of this series (part 1—this article) deals with the investigation of the thermophysical properties of the salt fuel system, criticality search and neutron-flux energy spectrum. An identical typical design of the MSFR core has been considered for a neutronic simulation by using MCNPX V2.7 based on the chemical composition of the fuel salt mentioned in both projects. The thermophysical evaluation has been conducted through literature research and theoretical methods based on the experimental values for the salt component properties. The results of the study are presented for thermophysical properties, including the melting point, vapour pressure/boiling point, specific heat capacity, thermal conductivity and density, in addition to neutronic simulation for the core critical dimension and neutron-flux spectrum of both the chloride- and fluoride-based salt fuel systems. In the discussion of the results, it is concluded that both the chloride and fluoride salt fuel systems have benefits that are seen on different comparative parameters. The delivered data will provide future decision makers with evidence for the salt choice for balancing their design objectives with the opportunities and expectations. Thus, a final selection of the most appropriate salt fuel system to be used in MSFRs will be postponed for more investigation in the final part of this article series, combining the data with different potential user profiles.

Keywords: nuclear reactors; molten salt fast reactors; fuel salt; thermophysical properties; neutronic criticality; iMAGINE; EVOL



Citation: Noori-kalkhoran, O.; Litskevich, D.; Detkina, A.; Jain, L.; Cartland-Glover, G.; Merk, B. On the Employment of a Chloride or Fluoride Salt Fuel System in Advanced Molten Salt Reactors, Part 1: Thermophysical Properties and Core Criticality. *Energies* **2022**, *15*, 8865. <https://doi.org/10.3390/en15238865>

Academic Editor: Hiroshi Sekimoto

Received: 7 November 2022

Accepted: 21 November 2022

Published: 24 November 2022

Publisher's Note: MDPI stays neutral with regard to jurisdictional claims in published maps and institutional affiliations.



Copyright: © 2022 by the authors. Licensee MDPI, Basel, Switzerland. This article is an open access article distributed under the terms and conditions of the Creative Commons Attribution (CC BY) license (<https://creativecommons.org/licenses/by/4.0/>).

1. Introduction

Generation IV of the nuclear energy systems will provide sustainable energy generation that meets clean air objectives and provides long-term availability of systems and effective fuel utilisation for worldwide energy production [1]. All Generation IV systems aim at performance improvement, new applications of nuclear energy, and/or more sustainable approaches to the management of nuclear materials; however, with differing priorities.

Molten salt fast reactors (MSFRs) as one of the candidate systems, in addition to satisfying the Gen IV objectives, derive the benefit of operating in a “Closed Fuel Cycle”

mode without the extensive cost and challenges of solid fuelled systems [2]. This feature can solve the main Achilles' heel of nuclear power plants—waste management and its related environmental issues—with the ability to use light water reactors' (LWRs) spent fuel (SF) to fabricate the molten salt fuel for use in the reactor core. Furthermore, a high breeding ratio of MSFRs makes this reactor type one of the best selections for long-term energy extraction, even without the need for refuelling [3].

One of the main and most fundamental challenges in the design of MSFRs is to select the appropriate molten salt fuel, as it strongly influences the neutronic, thermal-hydraulic, life cycle, shielding, breeding ratio, structural damage parameters and structural material dedication for the reactor. It can be said that it is the most fundamental and effective parameter in the design of this type of reactor programme.

A salt fuel/coolant comprises different individual salt components mixed into a multi-component system, e.g., as binary or ternary mixtures, typically an alkali metal salt and a heavy metal fuel salt. The melting points of each salt component are generally too high for coolant applications, and mixing several components into the binary/ternary systems reduces the melting point of the resulting salt system to more practical levels [4].

Various salt fuel/coolant systems were proposed, along with different research and projects interested during the development periods of MSRs and pyro-reprocessing. One of the first successful projects was conducted by the Oak Ridge National Laboratory (ORNL) between 1965–1969, and different salt fuel systems were examined through the Molten Salt Reactor Experiments (MSRE) [5–7] and the integrated results were delivered in the report [8]. A quaternary fluoride-based salt fuel system “LiF-BeF₂-ZrF₄-UF₄ (65.0-29.1-5.0-0.9 mol%)” with 33% of ²³⁵U was considered in the ORNL studies for the first criticality, although different experiments were conducted later to recognise the best salt fuel composition. Another project was run by ORNL in 1972, designing a thermal-spectrum molten salt breeder reactor (MSBR) by employing LiF-BeF₂-ThF₄-UF₄ as the salt fuel (²³⁵U enrichments between 33–90%) to include both fissile and fertile materials in the fuel composition [9]. Asher et al. conducted a detailed assessment of a 2500 MWe molten chloride salt fast reactor for the UK with lessons learned from the MSRE project from 1971 to 1972 [10]. Their preliminary study had shown that a fast system using the ²³³U/²³²Th cycle and fluoride salts did not indicate encouraging results, thus they considered a new ternary salt fuel, “NaCl-UCl₃-PuCl₃” (60.0-37.0-3.0 mol%), for their project.

In the last years, during 2010–2014, the EVOL project (Evaluation and Viability of Liquid Fuel Fast Reactor System) was developed by CNRS (France), partly under a European Commission grant to innovate the molten salt fast reactor (MSFR) concept [11,12]. As a result of this, two different quaternary fluoride-based salt fuel systems, “LiF-ThF₄-UF₄-PuF₃ (78.6-12.9-3.5-5 mol%)” and “LiF-ThF₄-UF₄-(TRU)F₃ (77.5-6.6-12.3-3.6 mol%)”—with ²³⁵U enrichments between 5–30%, depending on the core design—were proposed to be used in the MSFR (TRU: transuranium elements, which are mainly represented by PuF₃). In addition, the EVOL team arranged a strong collaboration with the MARS project (minor actinides recycling in molten salts), supported by Russian agencies and ROSATOM [13]. The European and Russian partners have conducted theoretical and experimental studies to verify the feasibility of the MOSART [14] and MSFR systems with a different core focus. On the one hand, to reduce the long-lived waste toxicity, and on the other hand, to produce electricity simultaneously. EVOL has been followed by a later project funded by the Euro commission, entitled “SAMOFAR (A Paradigm Shift in Reactor Safety with the Molten Salt Fast Reactor)”, conducted during 2015–2019 [15]. The main goal of the SAMOFAR project is to evaluate the safety features of MSFRs for future applications. The ternary system of LiF-ThF₄-UF₄ (77.5-20.0-2.5 mol%) has been identified as one of the salt fuel candidates to be used in the MSFR in this follow-up project of EVOL. In addition to the past and ongoing projects in this field, some studies can be found through published literature as results of academic research. In one of the most recent studies, Faure and Kooyman [16] have analysed the application of bromide and iodide salts as potential nuclear salt candidates in MSRs. They have concluded the analogous application of iodide salts in comparison

to the fluoride and chloride ones, while bromide salt has less chance because of its high gamma emission. A review work has been published by Gakhar et al. to analyse the properties, purification and corrosion of salt fuel by focusing on the fluoride and chloride one recently [17].

The iMAGINE project of the University of Liverpool chased the idea of operating a reactor on spent fuel without prior reprocessing for energy production and waste management [3,18]. The more detailed investigation, “Defining a Draft for a Zero Power Reactor Experiment for Molten Salt Reactors,” was launched at the University of Liverpool in collaboration with other academic and company partners in June 2021 [19–24]. The project focuses on developing a zero-power molten salt fast reactor to study the iMAGINE approach experimentally as the first step into a nuclear system that can employ the spent nuclear fuel extracted from light water reactors (LWRs) as the main fuel source and operate as a closed fuel cycle. The ternary/quaternary (adding PuCl_3 , latest through breeding) chloride-based salt fuel system “ $\text{NaCl-UCl}_3\text{-UCl}_4$ ” with two different compositions of 42.5-17-40.5 mol% and 20-23.65-56.35 mol% was considered as the starting composition (it should be noted that this composition can be changed during projects based on new findings). The project is looking to analyse/optimize the design parameters in all aspects for a zero-power molten salt fast reactor as a first step on the Gen IV MSR ladder.

This manuscript starts the first part (part 1) of a series of studies on the full-scope evaluation of employing chloride or fluoride salt fuel in MSFRs from different perspectives. In this manuscript, as the first step of the series, the pros and cons of using chloride or fluoride salt fuel in MSFR designs are investigated from a thermophysical property and core criticality point of view. In order to be as realistic as possible, a one-to-one comparative study was conducted between the EVOL-proposed fluoride-based salt fuel and the chloride-based iMAGINE systems. In addition, a pile-type cylindrical salt fuel reactor was simulated by using MCNPX V2.7, and the criticality simulation results were used to support the comparison study. Finally, a comparative table is presented that points out the results of this evaluation for a better understanding of each salt system’s advantages and disadvantages.

2. Simulation

In order to implement an impartial comparison study, neutronic simulations of a cylindrical pile-type MSFR design were conducted by using the Monte Carlo code MCNPX V2.7 [25] with the ENDF/B-VII.1 cross-section library [26], similarly for both fluoride and chloride salt. The Monte Carlo N-Particle Transport code (MCNP) is a general-purpose Monte Carlo radiation transport code designed to track many particle types over broad ranges of energies [25]. Figure 1 depicts the simulation geometry and layout of the reactor core.

The reactor core has been simulated for two different salt fuel systems for the iMAGINE project (chloride-based) and one salt fuel system-resulting EVOL project (fluoride-based) [11]. Table 1 lists the material composition used for the simulation in the MCNPX code.

The exact composition of the stainless steel and Ni-based alloy reflector used in the simulation is listed in Table 2.

To cover the all-important parameters affecting the design, especially in the core material inventory and burnup during the time (will be covered in parts of this article series), various power levels of 1 kW, 10 kW, 100 kW, 1 MW, and 10 MW were considered in the calculations. This issue is very important, as some new poison/fissile material is generated at a higher power level (while it cannot be seen in a lower power, such as the 1 kW zero-power research reactors) and over longer operation periods, which can affect the comparison study.

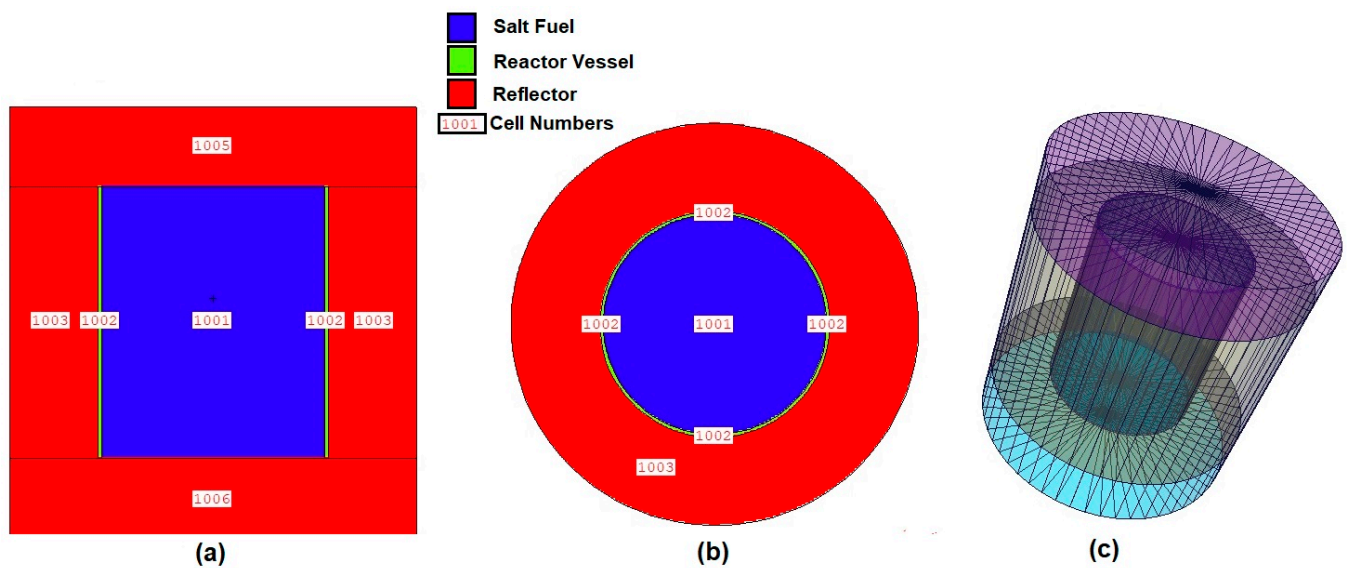


Figure 1. Configuration of simulated reactor core: (a) side view; (b) top view; (c) 3D wireframe view.

Table 1. Salt fuel systems were considered for iMAGINE and EVOL projects.

Reactor Type	Salt Fuel Composition	Reactor Vessel	Reflector
iMAGINE-Eutectic ¹	NaCl-UCl ₃ -UCl ₄ (42.5-17-40.5 mol%)	Stainless Steel	NaCl
iMAGINE-HMR ²	NaCl-UCl ₃ -UCl ₄ (20-23.65-56.35 mol%)	Stainless Steel	NaCl
EVOL	LiF-ThF ₄ -UF ₄ -PuF ₃ (78.6-12.9-3.5-5 mol%)	Ni-based alloy	Ni-based alloy

¹ Eutectic refers to the composition of the material in the Eutectic system point where the melting point of the ternary mixture is lower than the melting point of the constituents (for more, please refer to Section 3).
² HMR refers to the heavy metal-rich composition where the fraction of heavy metals has been increased in the salt system.

Table 2. Composition of stainless steel and Ni-based alloy applied in simulation (atom fraction).

Material	Cr	Mn	Fe	Ni	W	Mo	Ti
Stainless Steel	3.54×10^{-3}	8.74×10^{-3}	9.80×10^{-1}	7.60×10^{-3}	0	0	0
Ni alloy	8.01×10^{-2}	2.57×10^{-3}	6.32×10^{-3}	7.94×10^{-1}	9.98×10^{-1}	7.36×10^{-3}	2.95×10^{-3}
Material	C	Si	Al	B	P	S	
Stainless Steel	0	0	0	0	0	0	
Ni alloy	2.94×10^{-3}	2.52×10^{-3}	5.20×10^{-4}	3.30×10^{-4}	2.30×10^{-4}	4.00×10^{-5}	

The simulations have been conducted by using 1.0×10^6 particles ($NPS = 1.0 \times 10^6$) and 100 cycles, where the first 10 cycles will not be considered (inactive cycles), while the rest will be used as calculation-active cycles. These NPS and cycle values can reduce the standard deviation (ST Dev) of the calculations below 7.0×10^{-5} , a number which seems to be acceptable and reliable for this type of neutronic simulation study. The criticality temperature of the salt fuel was set to 980 K, based on the currently used operational temperature of MSFRs and the proposed temperature in the EVOL project's final report [11] and the data availability of the iMAGINE salt (930 K to 1030 K). In addition, a temperature gradient of 50 °C/K was considered in the contact surface of the salt fuel/reactor vessel and reflector in each order. In order to present the flux-energy spectrum, the energy range of $[1.0 \times 10^{-6}$ to $1.0 \times 10^{-3}]$, $[1.0 \times 10^{-3}$ to 1.0] and [1.0 to 5.0] MeV has been subdivided

equally into 400, 200 and 200 fine ranges, respectively. This segmentation of energy can maintain the ST Dev of flux in each range below 6.0×10^{-4} , which seems acceptable for this broad range. The reactor core volume was meshed, from $x = y = [-69 \text{ to } 69]$ and $z = [0 \text{ to } 170]$ cm, using 20 equal meshes in each direction (by using the Tmesh card) to visualise the flux distribution over the reactor core. Further information about the simulation procedure can be found in Section 3.2.

3. Results and Discussions

3.1. Thermophysical Properties of Salt Fuel

As has been mentioned previously, the thermophysical properties of the salt fuel are one of the most important elements in the design of an MSFR, as they can affect all the design parameters, from neutronic to thermal-hydraulic ones and, thus, form a key parameter in the safety of MSFRs. Table 3 summarises the key constraints in the selection of molten salt fuels.

Table 3. Key constraints of molten salt fuel.

Category	Constraint
Physical	Low melting point
	High boiling temperature
	Low vapour pressure
Chemical	Solubility of fissile and fertile material
	Less production of hardly manageable isotopes
	Less clean-up of the fuel salt during reactor's life cycle
	Less corrosion potential
Thermal-hydraulic	High Specific heat capacity and thermal conductivity
Neutronic	Neutron transparency
	Irradiation resistance

Figure 2 shows the thermodynamic liquid projections of the (a) NaCl-UCl₃-UCl₄ [27] and (b) LiF-ThF₄-PuF₃ [28] salt fuel system, as applied in the iMAGINE and EVOL projects, respectively.

3.1.1. Melting Point

As has been mentioned in Table 3, the lower melting point of salt fuel, in addition to reducing the operating temperature of the MSFR, can mitigate structural corrosion, reduce the risk of freezing and improve safety factors. Figure 2a depicts the peritectic and eutectic points of the NaCl-UCl₃-UCl₄ salt system (iMAGINE project) at 432 °C (~705 K) and 338 °C (~611 K) and at 49.0-21.5-29.5 and 42.5-17-40.5 mol% compositions, respectively [27]. The peritectic points describe the temperature and composition points where a new solid phase can be formed (as a mixture of others), while the eutectic points determine the temperature and composition point where the maximum number of phases is in equilibrium. Moreover, the eutectic point shows the lowest possible melting point of a mixture that is applicable in the salt fuel system of an MSFR. Figure 2b and Table 4 show the phase diagram and invariant equilibria of the LiF-ThF₄-PuF₃ salt fuel system (EVOL project). It can be found that the peritectic and eutectic points of the EVOL salt system can happen at 590 °C (~863 K) and 549 °C (822 K) and at the 69.2-28.3-2.5 and 72.4-25.3-2.3 mol% compositions, respectively (eutectic values were reported as 817 K and 74.9-22.3-2.8 mol% in the EVOL final report [11,28]). Regarding the peritectic and eutectic temperature and molar composition for both the iMAGINE and EVOL salt systems, some important points can be investigated: (i) In addition to the thermophysical properties of the salt system, the neutronic criticality of the reactor core can change/dictate the portion of fissile/fertile

material in the mixture. It means that the above-mentioned molar composition needs to be recalculated with respect to the required amount of fissile/fertile material to form a critical core, although it is demonstrated that the mentioned temperature and compositions will still be the closest values in the finalised critical core. (ii) The temperature gradient that exists between the peritectic and eutectic composition for the iMAGINE and EVOL salt fuel systems is 94 and 41, respectively, which as much as a higher gradient between the peritectic and eutectic points can keep the ternary mixtures as a single phase in a wider range. Therefore, the higher gradient for the iMAGINE salt fuel system can benefit the application in MSR. (iii) The most important point of this investigation is the possibility of a lower working temperature of the molten salt reactor core in the iMAGINE project in comparison to EVOL due to their eutectic melting points of 338 °C (~611 K) against 549 °C (822 K), respectively, that add the above-mentioned benefits to the salt fuel system and reactor operation.

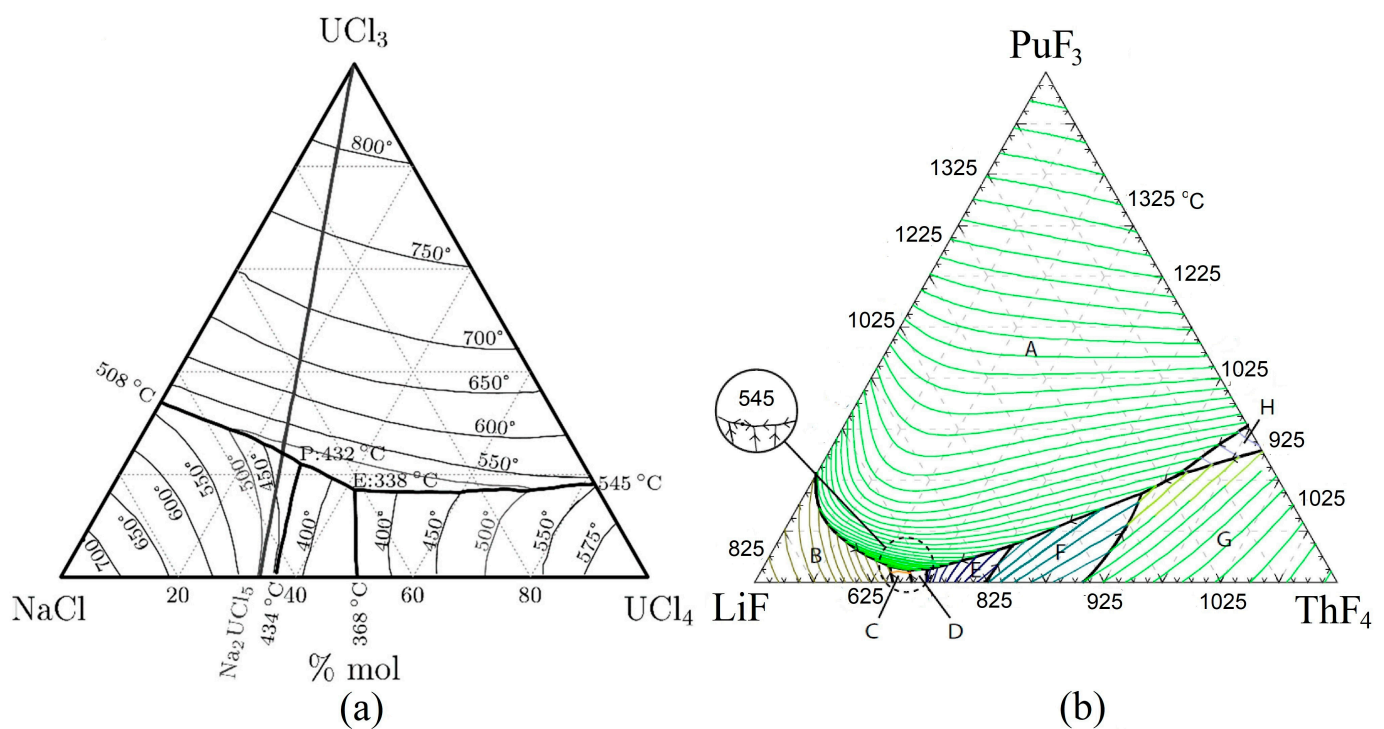


Figure 2. Thermodynamic liquid projections of (a) NaCl-UCl₃-UCl₄ and (b) LiF-ThF₄-PuF₃ (primary crystallisation phase fields: (A) (Pu,U) F_x (ss); (B) LiF; (C) Li₄UF₈; (D) Li₇U₆F₃₁; calculated Li₄U₄F₁₇; (F) UF₄; (G) PuU₂F₁₁).

Table 4. Invariant equilibria and saddle point of LiF-ThF₄-PuF₃ salt fuel system.

LiF	ThF ₄	PuF ₃	Temperature (K)/Equilibria Type	Crystal Phase in Equilibrium
0.692	0.283	0.025	863/Quasi-Peritectic	(Th,Pu) F _x (s.s.), LiTh ₂ F ₉ , LiThF ₅
0.724	0.253	0.023	822/Eutectic	(Th,Pu) F _x (s.s.), LiThF ₅ , Li ₃ ThF ₇

3.1.2. Boiling Point and Vapour Pressure

The molten salt fuel system's vapour pressure shows its tendency to change the phase into a gas state. Similar to other substance systems, this value is a direct function of temperature and increases with the temperature rise. In addition, the boiling point is an inverse function of vapour pressure. For both the neutronic and thermal-hydraulic (TH) designs of MSFRs, vapour pressure can affect the parameters, jeopardise the reactor design calculations completely and even affect the accident source term and, as a result, the safety of the reactor core. A high vapour pressure led to an increase in the void inside the molten salt and subsequently affected the neutronic parameters of the core and TH

parameters of heat removal. Thus, the investigation of the vapour pressure (and, as a result, boiling point) of the salt fuel system in MSFRs is one of the key parameters in their design and safety assessment. Reactor designers and regulators try their best to maintain the design completely away from the boiling points of reactor material, including fuel and coolant (exclude the BWR reactors, where coolant needs to be vaporised). After careful consideration of the previously published literature, although experimentally measured values of NaCl, UCl₃ and UCl₄ were reported individually in rare publications, the core challenge still remains that a systematic study has not been performed for the purpose of considering the whole combined salt system, at least to our current knowledge. The main reason could be the higher interest in the fluoride-based salt fuel systems (and the requirement of data for the reactor operation of the MSRE) in comparison to chloride-based ones for MSRs. To tackle this issue, Raoult's Law was used to calculate the vapour pressure of the salt system based on the components' substances. The law states that the vapour pressure of a mixture is the sum of the vapour pressures of the individual components multiplied by their molar fraction:

$$P_{total} = \sum P_N \times X_N \quad (1)$$

where P_N is the vapour pressure of a liquid within the mixture, X_N is the Molar fraction of a liquid within the mixture, and as a result, P_{total} is the determined vapour pressure of the mixture. It should be noted, however, that the composition of the vapour phase will not be the same as the liquid phase, as different masses of composed substances will escape from the liquid mixture to the headspace based on the individual vapour pressure of each component. The experimental values of vapour pressure for the iMAGINE salt fuel system components, including NaCl, UCl₃ and UCl₄, were collected in a different range of temperatures (based on availability) and compared for accuracy among previously published works [29–36]. The EVOL salt fuel system vapour pressures were extracted from the EVOL final report [11]. Figure 3 shows the vapour pressure profiles for each salt fuel system component individually and in total. As can be seen in this figure, the individual vapour pressure of the iMAGINE salt fuel system components is higher in some order of magnitude in comparison to the EVOL one (Figure 3a,b).

In addition, Figure 3c shows the comparison of the iMAGINE (Eutectic and HMR) and EVOL salt fuel systems' vapour pressure in an available range of temperatures (and likely operational temperature range) in more detail. This figure confirms that the total vapour pressure for the iMAGINE project fuel is higher than the EVOL one by some order of magnitude. The total vapour pressure calculated for the likely output temperature of the MSFR (~1000 K) is about 0.07 Pa for the EVOL project, while this value can be found at 88.0 and 122.4 Pa for the iMAGINE eutectic and HMR, respectively. As can be seen in Figure 3b, UCl₄ has the highest vapour pressure compared to the other components of both salt fuel systems, and it shows the importance of conservative treatment for this substance as one of the fuel salt elements.

3.1.3. Specific Heat Capacity

The specific heat capacity (heat capacity in the mass unit of a substance— C_p) is one of the main factors that can directly affect the thermal-hydraulic and indirect neutronic parameters of a reactor (by influencing the temperature profile of a reactor's material/salt fuel). The higher heat capacity of a fuel system can be one of the benefits of a nuclear reactor core, as it is proportional to the amount of heat that can be stored in the fuel (and salt fuel system in MSRs). On the other hand, it can alter the fuel system temperature rise regarding heat generation. Higher C_p can tolerate the energy production smoother and, as a result, soften the change in neutronic parameters through feedback effects. Moreover, the safety margins of the salt fuel system in the case of a power transient are a direct function of specific heat capacity, and it grows with increasing the C_p , providing longer grace or reaction periods due to the slower temperature rise at a given power. These show the importance of this factor in the safe, reliable and efficient operation of the reactor core. It

can be added that a higher heat capacity can clearly increase the heat transfer efficiency in the heat exchanger and the steam generators and, as a result, rise the efficiency of the whole system. Similar to the other thermophysical parameters of molten salt fuels, a few studies can be found in the literature that reposted a specific heat capacity of salt fuel systems, such as NaCl-UCl₃-UCl₄ and LiF-ThF₄-UF₄-PuF₃. Since the salt system will progress during the operation due to the fission products that will be dissolved, this parameter will sure need to be investigated to the last details in an experimental reactor with real power production.

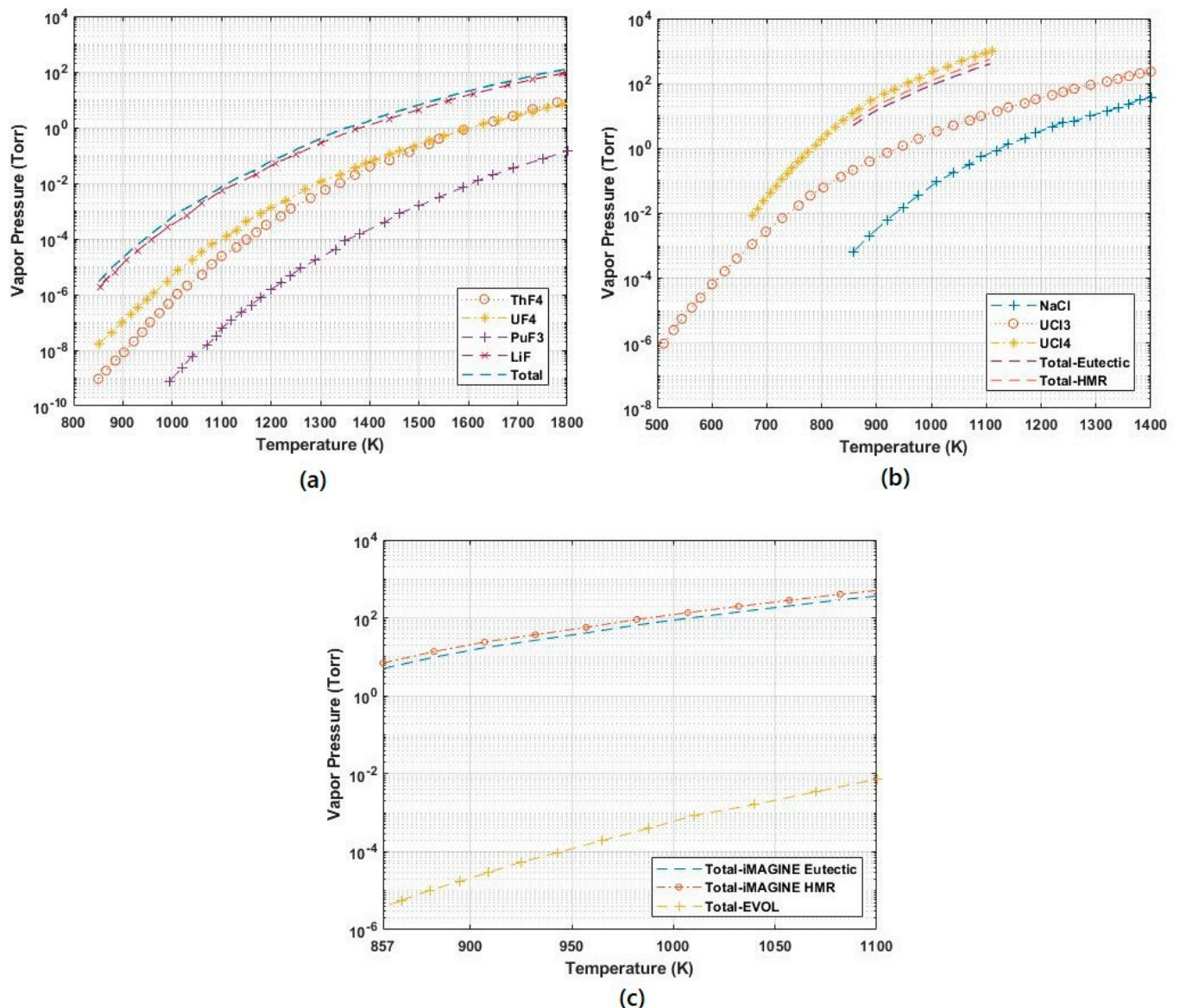


Figure 3. Total and components vapour pressure of salt fuel system for (a) EVOL, (b) iMAGINE and (c) comparison between EVOL and iMAGINE project in the range of 857–1100 K.

One of the best shortcuts in this situation is to evaluate the components of the salt fuel system individually and try to spot the estimation of system-specific heat by employing the Neumann–Kopp rule (NKR) [37,38]. The rule (in original terms, the law) was first presented by Kopp in the following form: “Each element has essentially the same specific or atomic heat in compounds as it has in the free state”. Mathematically, the NKR can be expressed as follows: If a solid compound $A_aB_bC_c$ is formed from solid elements A, B and C by the reaction



based on the NKR, the specific heat capacity of $A_aB_bC_c$ can be obtained by

$$C_{p,m}(A_aB_bC_c,s) = aC_p(A,s) + bC_p(B,s) + cC_p(C,s) \tag{3}$$

where $C_{p,m}$ determines the heat capacity of the mixture; a , b and c are a molar fraction of A , B and C in the mixture; and $C_p(x,s)$ shows the heat capacity of substance “ x ” in solid-state, respectively. A systematic survey cannot be found in the EVOL final report [11] about the specific heat capacity and its temperature dependence for the LiF-ThF₄-UF₄-PuF₃ salt system. They have just reported the value of 87.8 J/(mol·K) for the EVOL salt fuel system, regardless of the temperature change (constant to temperature) [11].

In this study, the specific heat capacity and its temperature functionality for the individual components of the salt fuel system have been extracted by surveying different publications for both the EVOL and iMAGINE projects [28–30,36,39–41]. Figure 4a,b depicts the specific heat capacity for the single components of the EVOL and iMAGINE salt fuel system, respectively, for both the solid and liquid phases.

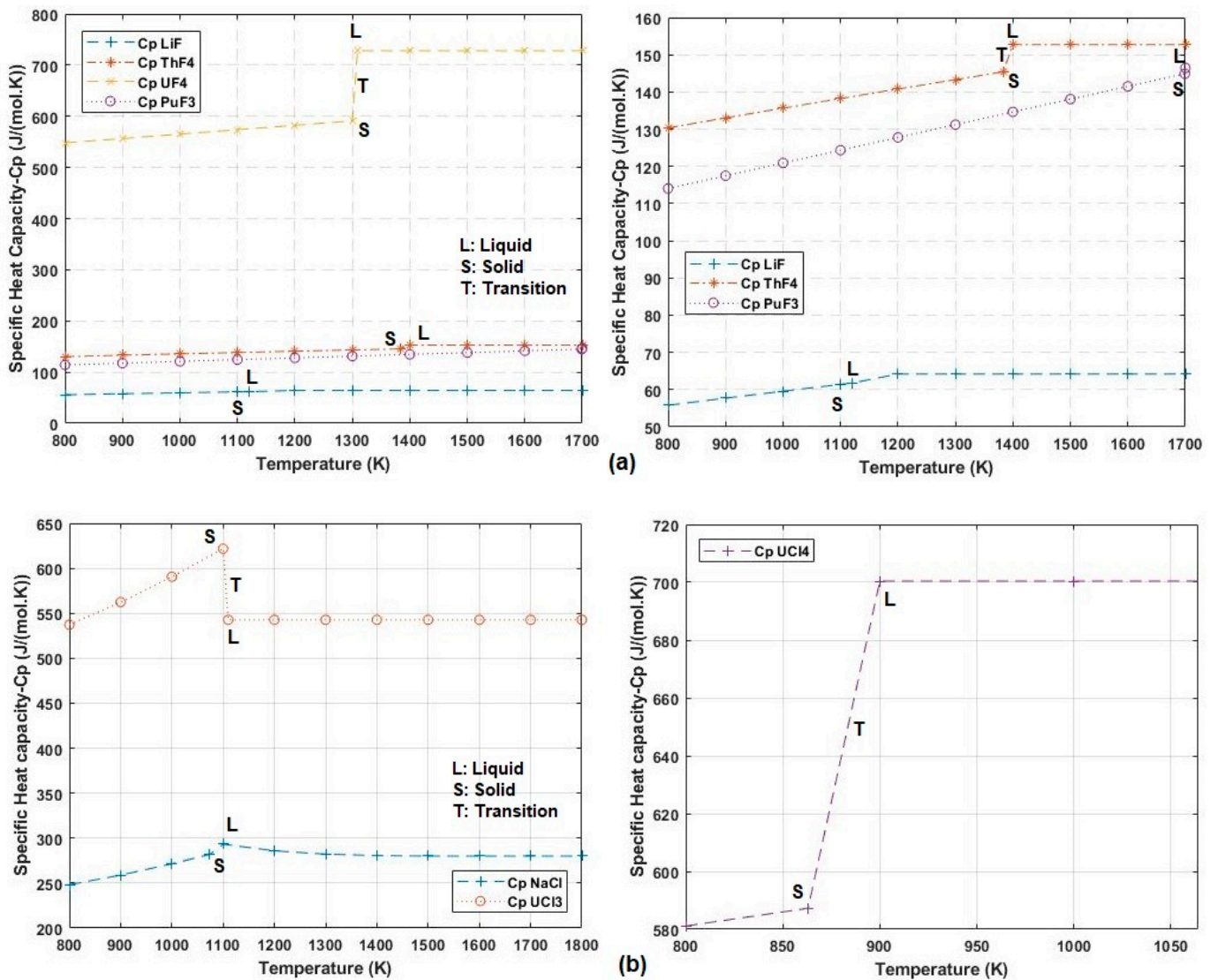


Figure 4. Specific heat capacity of (a) EVOL and (b) iMAGINE salt fuel system components [28–30,36,39–41].

For ease of observation, various axis ranges were depicted for the right and left sub-figures to show the details and make a clear comparative study. Different substance

phases have been mentioned by using L, S and T for the liquid, solid and transition phases, respectively. As can be seen in these figures, and it is mentioned through the references, C_p has an ascending behaviour with temperature for both salt fuel systems in the liquid phase (excluding UCl_3), although it has smooth alterations for the EVOL fuel, while it shows sharper changes for some of the iMAGINE components. In agreement with other studies, the specific heat capacity stays almost constant after the melting point, although it has step changes, usually in the transition phase. Both UF_4 and UCl_4 have distinguished treatment in the transition phase and make a large step at this point. One of the most important points is that the boiling point of all components of both salt fuel systems, except UCl_4 , are in the range of [1600–2230 K] (refer to Figure 3), while this value is about 1064 K for UCl_4 and shows the sensitivity of the iMAGINE salt fuel system and the important role of the specific heat capacity to alterations in the large range of the reactor core temperature. Finally, using the Neumann–Kopp rule, the specific heat capacity of the iMAGINE salt fuel system ($\text{NaCl-UCl}_3\text{-UCl}_4$) was calculated as 494.9 and 579.0 J/(mol·K) for the eutectic and HMR, respectively, and 87.9 for the EVOL project (which is in good agreement with 87.8 J/(mol·K), reported in the EVOL final report) in the liquid phase (constant specific heat). As mentioned above, the almost five times higher specific heat capacity of the iMAGINE (chloride-based) salt fuel system in comparison to EVOL plays an important role in defining the safety margins, the thermal-hydraulic of the system and, as a result, the neutronic and safety design parameters of this reactor core, although the low boiling temperature of UCl_4 needs to be considered in the calculations and in the definition of the limits for safe operation.

3.1.4. Thermal Conductivity

The thermal conductivity of molten salt is the most difficult fluid property to measure, and it has led to a large amount of confusion and error in heat-transfer calculations [36]. Previously published values for the thermal conductivity of molten salts and their components had overestimated the values, creating a source of error in the design, modelling and simulation of the TH behaviour of MSR. Two more reliable methods are usually employed to measure the thermal conductivity experimentally: the hot-wire and annular cylinder methods [42]. Unfortunately, there are neither systematic studies nor a comprehensive thermophysical properties database that present the thermal conductivity of ternary or quaternary salt fuel systems, although some useful information can be found for the unary and binary salt systems, such as LiF, NaF+KF, etc., [39,43–45]. One of the solutions for this lack of knowledge about the thermal conductivity of molten salts is by using theoretical models that have a maximum proximity to the experimental ones. By looking into the publication and references, it can be found that one of the best estimation models for molten salt thermal conductivity was presented by Rao and Turnbull [36,43,46]:

$$\text{Thermal Conductivity } (k) \left(\frac{\text{Watt}}{\text{m} \cdot \text{K}} \right) = 0.119 \times MPT^{0.5} \times \nu^{0.667} / \left(\frac{M}{n} \right)^{1.167} \quad (4)$$

where MPT is the melting point of the salt system, ν is the molar volume, M is the average formula weight of the salt ($\sum x_i M_i$), and n is the number of discrete ions per salt fuel system. The outcomes of this model have one of the best agreements with the experimental results of thermal conductivity, although it should be noted that this model has the sensitivity to the reasonable selection of n in the formula. Applying Equation (4) on the iMAGINE salt fuel system (Eutectic and HMR) (by selecting $MPT_{\text{Eutectic}} = 611$ K, $MPT_{\text{HMR}} = 735$ K, $\nu_{\text{Eutectic}} = 73.49$, $\nu_{\text{HMR}} = 86.73$, $M_{\text{Eutectic}} = 236.6$, $M_{\text{HMR}} = 306.3$ and $n = 3$) can give the values of 0.3163 and 0.2611 watt/(m·K), respectively. The same procedure on the EVOL salt fuel system ($MPT = 822$, $\nu = 19.87$, $M = 85.89$, and $n = 5$) also results in the value of 0.9078 watt/(m·K), which is in reasonable agreement with the 1.22 watt/(m·K) in the EVOL final report [11]. Some important points need to be considered in such calculations: (i) The model presented in Equation (4) is basically for one component salt, such as LiF, but lately, it has been found that it can be extended to multi-component salts and provides still

reasonable results. (ii) Based on the experiments, the thermal conductivity of a salt system is, in general, lower than the molar weighted average of its components. (iii) The really accurate values for thermal conductivity of the iMAGINE and EVOL salt fuel systems have to be obtained by direct experiments on the exact salt composition. Considering the above-estimated values of thermal conductivity, this indicates more efficient EVOL salt heat transfer properties in comparison to the iMAGINE one, although the most accurate benchmarking has to result from future experimental values of these parameters. Higher thermal conductivity of salt fuel systems can be a benefit in the efficiency of heat removal systems and safety margins in transient situations.

3.1.5. Density

Density, or the change in density as a result of temperature changes, is one of the most important parameters of MSR that can affect the neutronic parameters directly and indirectly and alter the specific heat capacity of salt fuel for thermal-hydraulic calculations. Specifically, the determination of density as a function of temperature is vital, as it will be applied to the calculation of thermal feedback and other neutronic parameters. It is one of the properties that can be measured straightforwardly and with high accuracy using the available experimental setups. As an accepted scientific rule that has great agreement with experiments, the density of most substances can be a linear function of temperature, at least for a reasonable temperature range:

$$\rho(T) = a - b \times T \quad (5)$$

where ρ is the density to be determined in gr/cm^3 , T is the temperature in Kelvin, and a and b are the two constants of this equation that need to be calculated [47]. On the other hand for the majority of molten salt mixtures and the molar volumes of the mixture can be tabulated in very good agreement as a linear function of mole fraction and molar volume of the pure components [48]. This means

$$V_{mixture}(T) = x_1 V_1(T) + x_2 V_2(T) \dots + x_n V_n(T) \quad (6)$$

where $V_{mixture}$ and V_1 to V_n is the molar volume of the mixture and its component with a dependence on temperature, respectively, x_1 to x_n are molar fractions of the components, and n is the component's number of salt fuel systems (all in temperature T (K)). As density is an inverse function of temperature, so one can write

$$\rho(T) = \frac{\sum x_i M_i}{V_{mixture}(T)} \quad (7)$$

where M_i is the molecular weight of salt component i . Based on Equation (7), using two different temperatures (T) to calculate $\rho(T)$, we can deliver an estimate for the parameters a and b in Equation (5) and, as a result, the linear function of the salt fuel system with temperature for the considered temperature range. Extracting the molar volume of the different components of the iMAGINE and EVOL salt fuel systems (at $T = 600$ and 800 °C) and using Equations (5) and (7) result in the following density function of temperature in Table 5.

Figure 5 depicts the calculated and reference values of the density function as a function of temperature for comparison. As it is indicated in this figure, the calculated results of this study, based on molar volume theory, and the references, are in good agreement in both, including the values and line slope, although minor discrepancies can be found in the line slope for the iMAGINE-HMR calculated and reference values. The EVOL salt fuel density is almost 9% and 27% higher than the iMAGINE-HMR and Eutectic, respectively, in the 600–800 °C (~873–1073 K) temperature range, which is considered as the operating temperature of MSRs in the case of industrial operation. A higher density has a direct effect on the neutronic calculations, as well as the thermal-hydraulic setting points. The macroscopic cross-sections in the neutronic calculation are proportional to the density

(exactly atomic density); thus, this parameter can affect the criticality and other neutronic parameters, which then would have to be compensated by a larger volume for the core and the flow in the heat transfer system. Even the slopes of the density function (here linear) are important in the dynamic behaviour of the reactor core (during a transient), as lower density gradient changes will lead to more stable behaviour of the reactor core against temperature changes. The density profile slope values for EVOL and iMAGINE-Eutectic look very close; only the iMAGINE-HMR system has a slightly sharper slope in comparison to the others.

Table 5. Calculated density functions as temperature for EVOL and iMAGINE salt fuel systems [47,48].

Salt Fuel	Density Function (600–800 °C; ~873–1073 K) (gr/cm ³)
EVOL	$5.1720 - 0.9223 \times 10^{-3} T$ (calculated in this study)
	$5.1550 - 0.8331 \times 10^{-3} T$ [11]
iMAGINE-Eutectic	$4.1224 - 1.0117 \times 10^{-3} T$ (calculated in this study)
	$4.2368 - 1.0256 \times 10^{-3} T$ [21,49]
iMAGINE-HMR	$5.1487 - 1.4316 \times 10^{-3} T$ (calculated in this study)
	$5.3995 - 1.8646 \times 10^{-3} T$ [21,49]

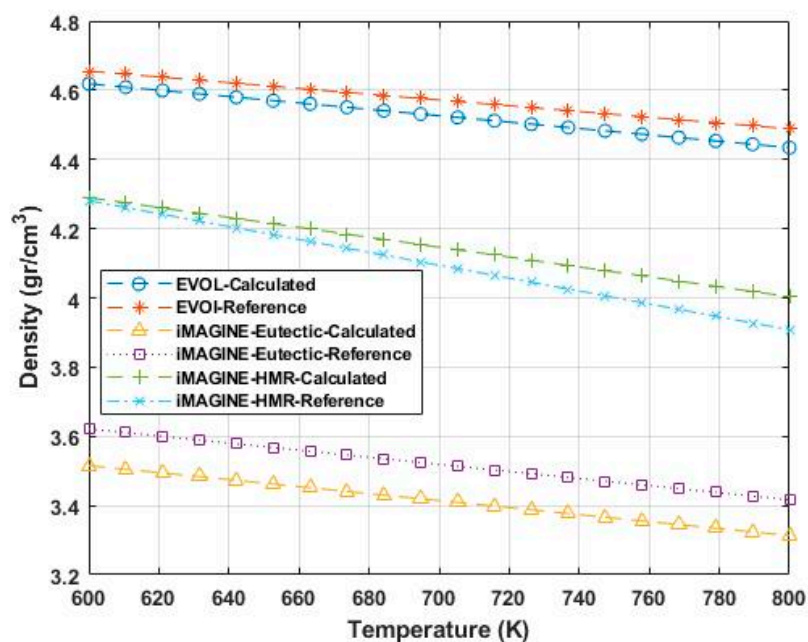


Figure 5. Density functionality of temperature for EVOL and iMAGINE salt fuel systems.

3.2. Criticality Search

The main purpose of the criticality search in a reactor core design is to keep the multiplication factor almost as a unit ($k_{eff} \sim 1$) by determining the dimension (geometry search) and even composition (composition search) of the reactor core. In the MSFRs, other important design parameters, such as the breeding ratio and neutron-flux energy spectra, come into account, making this more complicated. In order to achieve this goal and keep the comparative character of this study, some new criteria need to be defined for the criticality search procedure of MSRs in alignment with the EVOL outcomes. These criteria of the criticality search can be listed as follows:

- i. The reactor core geometry needs to be considered cylinder, as results of the EVOL survey [11] and different geometries, such as cylinder, sphere etc., have been surveyed in both the iMAGINE and EVOL projects.

- ii. The thermal-hydraulic design of MSRs can force the geometrical dimension of the reactor core, especially for the iMAGINE project, in which the main goal in the first step is to design a zero-power research reactor and remove heat by natural convection without having a specific heat transfer system, and thus, relying on leakage and low power. These criteria lead to having a vertical cylinder, which means, at the most, the diameter of the cylinder should be equal to or smaller than the cylinder height. These criteria come from the TH point of the natural convection source based on the density gradient in the reactor core (and can be connected by the Grashof (Gr) number).
- iii. Excess reactivity of 300–600 pcm is usually considered for this type of reactor to have enough criticality margin during the reactor's life cycle, although this value depends mainly on the burnup and core temperature history that will be studied in the next section of the article.
- iv. With a smaller reactor core, less fuel and lower fuel costs occur.

Criticality searches based on the above-mentioned criteria have been conducted by using an iterative simulation cycle. As values of k_{eff} are closer to the unit (in the range of 1.00+300 pcm and 1.00+600 pcm by considering the excess reactivity margin), narrower changes happen in the values of the dimensions to find the almost exact critical dimensions of the core. In order to ease this process and limit the cost of calculations, after some simulation cycles, the height of the reactor cylinder was fixed at 170 cm, with a vessel thickness of 2 cm using stainless steel/Ni alloy, based on the EVOL project [11,23]). In addition, it has been concluded that considering the 55 cm thickness of the reflector can make more efficient criticality in comparison to the 50 cm previously reported by Merk et al. [23]. Figure 1 shows the simulated reactor core geometry in MCNPX, and criticality search tables have been presented along Tables 6–8 for the iMAGINE-Eutectic, iMAGINE-HMR and EVOL salt fuel systems, respectively.

Table 6. Criticality search results for iMAGINE-Eutectic salt fuel system.

Type	V *- Height (cm)	V-IR/ID (cm)	V-ER/ED (cm)	Ref-ER (cm)	V-Volume (cm ³)	U235 (%)	Fuel T ** (K)	K eff	St Dev (%)
Eutectic	170	65/130	67/134	122	2.26	35	980	0.98021	0.00006
Eutectic	170	67/134	69/138	124	2.40	35	980	0.99286	0.00006
Eutectic	170	69/138	71/142	126	2.54	35	980	1.00492	0.00004
Eutectic	170	71/142	73/146	128	2.70	35	980	1.01658	0.00006
Eutectic	170	73/146	75/150	130	2.85	35	980	1.02772	0.00007
Eutectic	170	75/150	77/154	132	3.00	35	980	1.03847	0.00006

* V = vessel, IR = internal radius, ID = internal diameter, ER = external radius, ED = external diameter, Ref = reflector, St Dev = standard deviation, ** T = temperature (K).

Table 7. Criticality search results for iMAGINE-HMR salt fuel system.

Type	V *- Height (cm)	V-IR/ID (cm)	V-ER/ED (cm)	Ref-ER (cm)	V-Volume (cm ³)	U235 (%)	Fuel T ** (K)	K eff	St Dev (%)
HMR	170	63/126	65/130	120	2.12	35	980	1.04152	0.00007
HMR	170	61/122	63/126	118	1.99	35	980	1.02787	0.00005
HMR	170	59/118	61/122	116	1.86	35	980	1.01353	0.00006
HMR	170	58/116	60/120	115	1.80	35	980	1.00611	0.00005
HMR	170	57/114	59/118	114	1.73	35	980	0.99863	0.00007
HMR	170	55/110	57/114	112	1.61	35	980	0.95521	0.00007

* V = vessel, IR = internal radius, ID = internal diameter, ER = external radius, ED = external diameter, Ref = reflector, St Dev = standard deviation, ** T = temperature (K).

Table 8. Criticality search results for EVOL salt fuel system.

Type	V *- Height (cm)	V-IR/ID (cm)	V-ER/ED (cm)	Ref-ER (cm)	V-Volume (cm ³)	U235 (%)	Fuel T ** (K)	K eff	St Dev (%)
EVOL	170	61/122	63/126	118	1.99	35	980	1.05475	0.00007
EVOL	170	59/118	61/122	116	1.86	35	980	1.04632	0.00007
EVOL	170	57/114	59/118	114	1.73	35	980	1.03732	0.00007
EVOL	170	55/110	57/114	112	1.61	35	980	1.02764	0.00007
EVOL	170	53/106	55/110	110	1.50	35	980	1.01708	0.00006
EVOL	170	51/102	53/106	108	1.39	35	980	1.00551	0.00006

* V = vessel, IR = internal radius, ID = internal diameter, ER = external radius, ED = external diameter, Ref = reflector, St Dev = standard deviation ** T = temperature (K).

It is worth noting that these tables only list the closest iterations to the critical points, while the criticality searches have been conducted along a wider range. In each case, the simulated critical dimensions that most justify the criteria points have been highlighted in bold.

Finally, Table 9 compares the critical dimension of the reactor core for three fuel salt systems. It can be found from this table that the EVOL fuel salt system can justify the criticality criteria almost with 83% and 29% smaller volumes in comparison to the iMAGINE-Eutectic and HMR systems, respectively.

Table 9. Comparison of the critical dimension between three salt fuel systems.

Type	V *- Height (cm)	V-IR/ID (cm)	V-ER/ED (cm)	Ref-ER (cm)	V-Volume (cm ³)	U235 (%)	Fuel T ** (K)	K eff	St Dev (%)
iMAGINE-Eutectic	170	69/138	71/142	126	2.54	35	980	1.00492	0.00004
iMAGINE-HMR	170	58/116	60/120	115	1.80	35	980	1.00611	0.00005
EVOL	170	51/102	53/106	108	1.39	35	980	1.00551	0.00006

* V = vessel, IR = internal radius, ID = internal diameter, ER = external radius, ED = external diameter, Ref = reflector, St Dev = standard deviation, ** T = temperature (K).

In addition, as could be expected (as HMR relies on the heavy metal-rich salt system), the HMR criticality volume is about 41% less than the eutectic one. On the one hand, as mentioned above, a smaller critical core can optimise the fuel fabrication cost in MSRs. On the other hand, TH design and instrument installation will be less complicated in bigger fuel vessels.

One of the main features of MSFRs is to obtain a fast spectrum of the neutron flux (hard spectrum) as the philosophy for the design and a key to allow using a closed fuel cycle with sufficient self-sustained breeding. As has been mentioned previously, to obtain the fine resolution flux-energy spectrum, the energy range [1×10^{-6} to 5] MeV has been divided into 800 energy domains with more pro rata weight in the lower energy groups. Figures 6–8 depict the flux-energy spectrum for each salt fuel system, and Figure 9 compares them in detail. It should be noted that all three profiles have been weighted to unit summation

$$\left(\sum_0^E flux = 1\right).$$

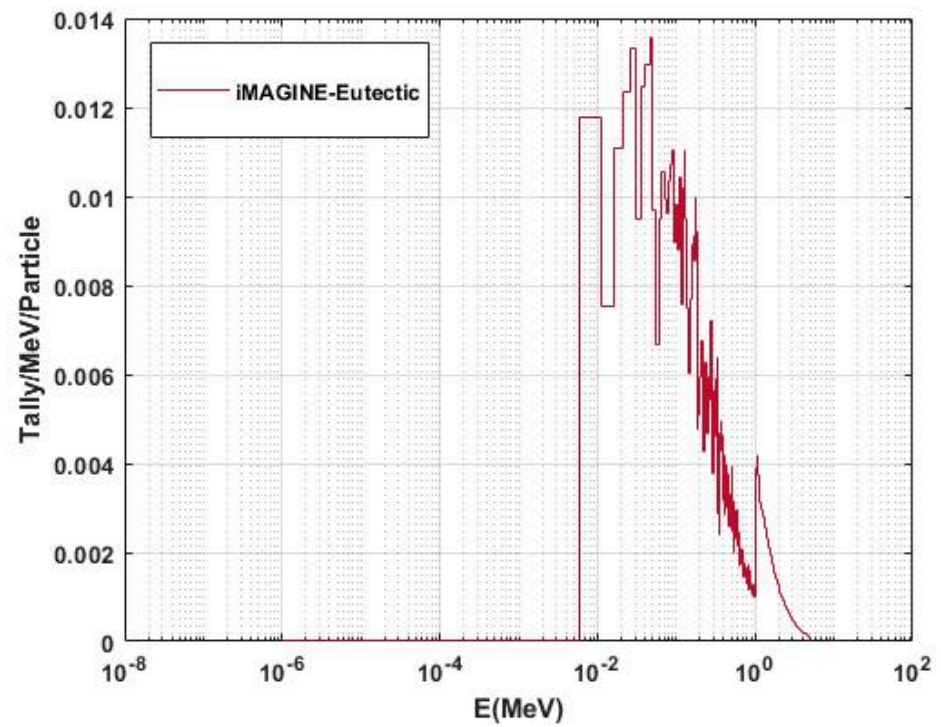


Figure 6. Neutron fluxenergy spectrum for iMAGINE-Eutectic salt fuel system.

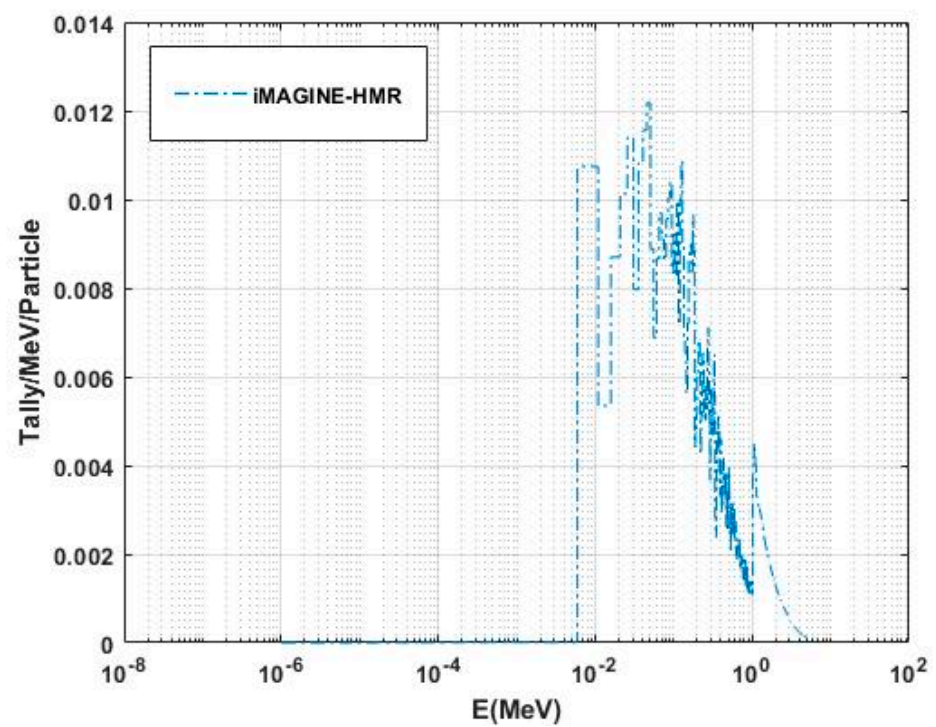


Figure 7. Neutron fluxenergy spectrum for iMAGINE-HMR salt fuel system.

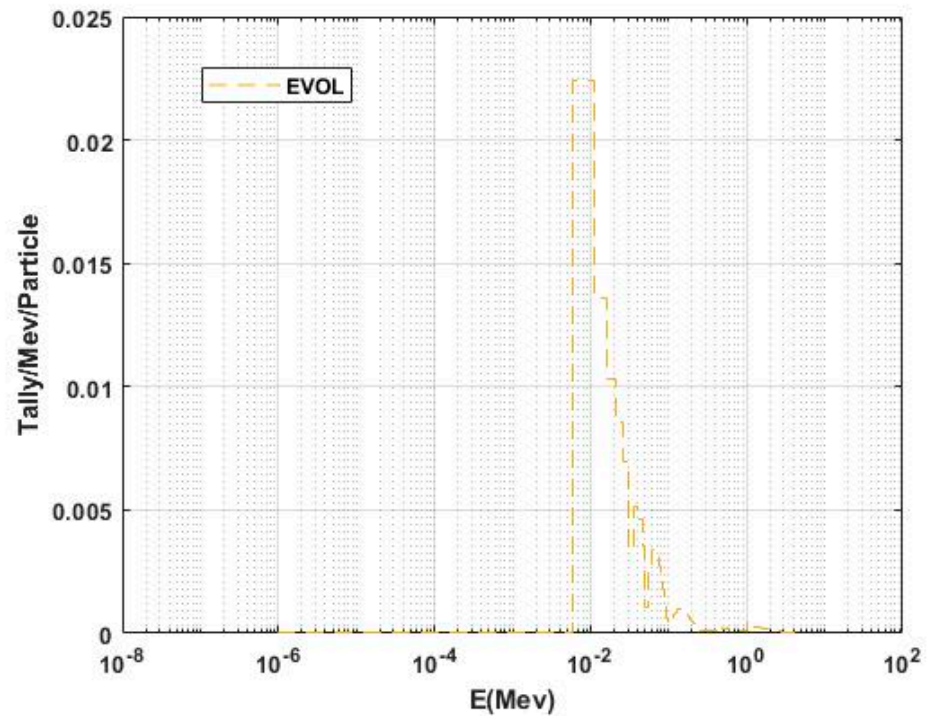


Figure 8. Neutron fluxenergy spectrum for EVOL salt fuel system.

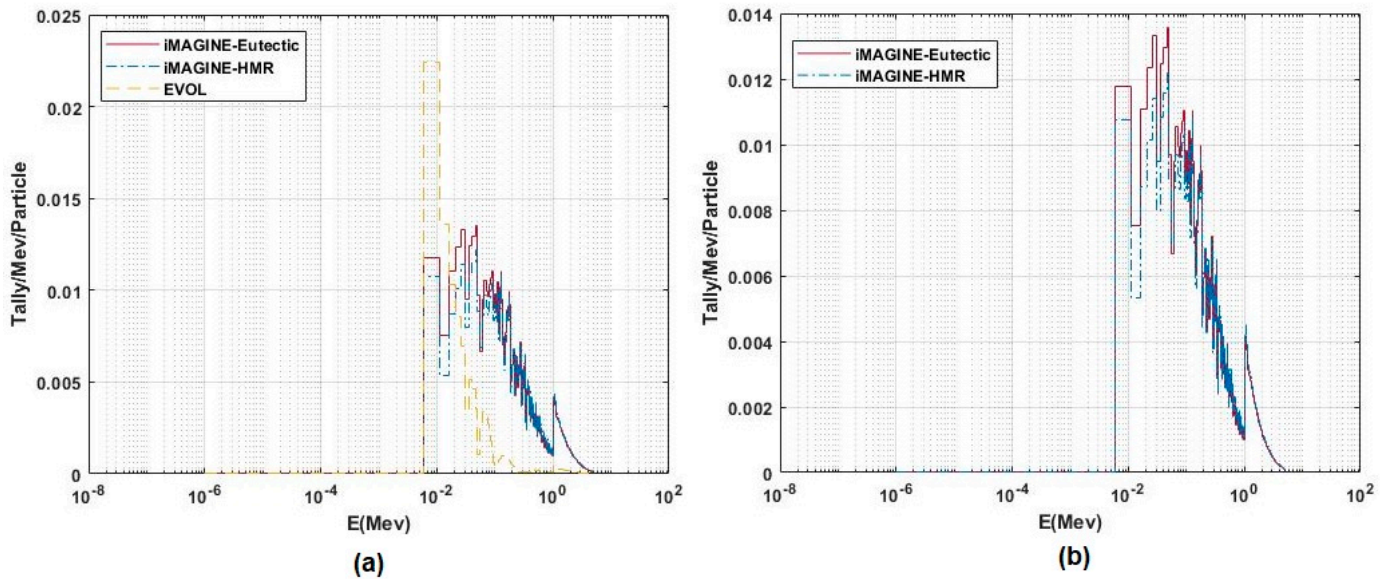


Figure 9. Comparative neutron-flux energy spectrum of iMAGINE and EVOL salt fuel systems.

As it can be seen in Figure 9a, both the iMAGINE-Eutectic and HMR systems have an almost similar flux-energy spectrum, qualitatively and quantitatively, with only a very slightly harder neutron spectrum for the HMR case (both the shape and amplitude in Figure 9b show this clearly); however, the EVOL salt fuel system generates significantly different flux-energy spectra in both shape and amplitude. To investigate the neutron spectrum in more detail, Figure 10 depicts the cumulative neutron-flux energy spectrum fraction for each salt fuel system. Every point on each profile shows the fraction of flux cumulated between the minimum energy of the spectrum (10^{-8}) to the energy of that point ($\int_{10^{-8}}^E Flux(E)dE$). Some energy ranges have been specified by a red coloured vertical line at $E = 0.01, 0.1, 1,$ and 5 MeV and the intersection of the profiles with energy lines, as indicated by the profile's colour.

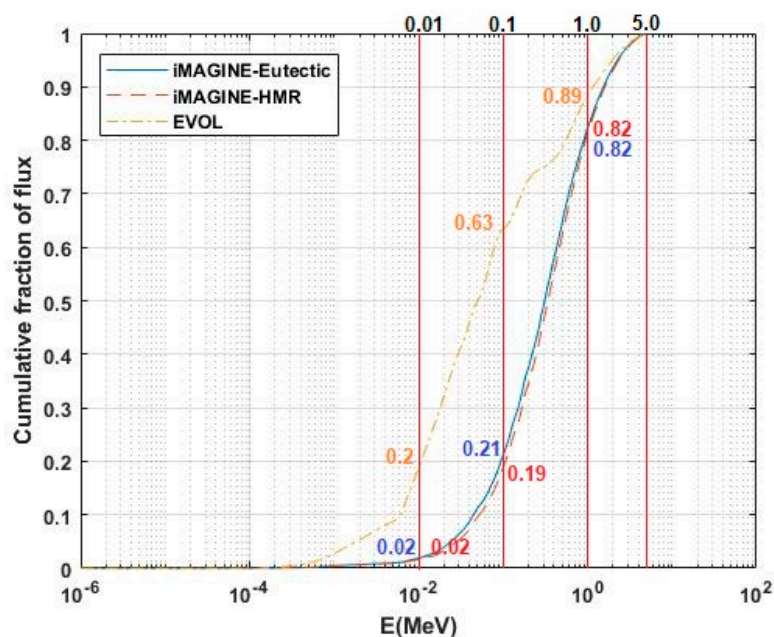


Figure 10. Cumulative fraction neutron-flux spectrum for iMAGINE and EVOL salt fuel systems.

For ease of use, some of the neutron-flux energy fractions are, in addition, listed in Table 10 (by subtracting the intersection points easily). As has been listed in this table, about 20% of EVOL's neutron flux has energies of less than 0.01 MeV ($E < 0.01$ MeV), while this value is around 2% for both the iMAGINE salt fuel combinations, Eutectic and HMR. In the energy range of [0.01 to 0.1] MeV, similar behaviour can be seen, while the fraction of neutron flux for iMAGINE-Eutectic and HMR are, respectively, 19% and 17%. EVOL shows almost 43% of its flux in this energy range (the highest flux fraction range for EVOL).

Table 10. Neutron flux-energy spectrum fraction in different energy ranges.

Fuel Salt System	$E < 0.01$ MeV	$0.01 < E < 0.1$	$0.1 < E < 1.0$	$E > 1.0$
EVOL (%)	20	43	26	11
iMAGINE-Eutectic (%)	2	19	60	19
iMAGINE-HMR (%)	2	17	63	18

In strong contrast, iMAGINE-Eutectic and HMR generate 60% and 63% of their neutron flux in the range of [0.1 to 1.0] MeV, while this value is only about 26% for the EVOL salt fuel system. It shows the specificity of the iMAGINE salt fuel system to EVOL, delivering as the highest portion of neutron-flux generations happen in a higher energy range, which is one of the main objectives of the MSFRs since this is one of the key parameters to assure sufficient breeding. Finally, about 11% of the EVOL neutron flux is in the range of $E > 1.0$ MeV, while this value is 19% and 18% for the iMAGINE-Eutectic and HMR systems. As a result, it can be concluded that the neutron energy spectrum in iMAGINE is significantly harder, as is clearly confirmed in Figure 10 and Table 10, where about 79% and 81% of iMAGINE-Eutectic and HMR neutrons are seen in the fast neutron energy range (considering $E > 0.1$ MeV or 100 keV as the fast energy threshold), while this value is only 37% for the EVOL salt fuel system.

4. Conclusions

The fourth generation of nuclear power plants has attracted high interest among industry and scientists because of their safety features and higher efficiency. Molten salt fast reactors (or, maybe, better named molten salt fast breeder reactors) are one of the most

attractive candidates among other design types, as in addition to their safety features, they can benefit from high efficiency, a high breeding ratio, and even work in an integrated closed fuel cycle [19]. Molten salt fuel systems for MSFRs are usually selected based on fluoride or chloride molten salts, and there is a scientific challenge between these two groups regarding the advantages and disadvantages of each. In the first part of this study, the thermophysical properties and neutronic criticality of both groups were investigated qualitatively and quantitatively. Table 11 summarises the highlighted results of this evaluation based on the EVOL (fluoride-based) and iMAGINE (chloride-based) salt fuel systems, although a comparison from other points of view and more evaluation will be discussed in the next parts of this publication series. In each parameter's case, the most favourite value from the MSFRs design perspective has been mentioned in bold. As this table shows, none of the salt fuel systems can justify all the criteria of design and safety in terms of salt fuel composition and criticality design. A full-scope conclusion will be presented in the last part of this series article, where all the design parameters have been investigated properly.

Table 11. Conclusion of thermophysical properties and neutronic criticality for EVOL (fluoride-based) and iMAGINE (chloride-based) MSFRs.

Parameter/Salt Fuel System	EVOL	iMAGINE-Eutectic	iMAGINE-HMR	
Thermophysical properties	Melting point (K) Figure 2 Higher melting point and Lower Peritectic/Eutectic gradient	Eutectic: 822 K (Composition: 72.4-25.3-2.3 mol%) Peritectic: 863 K (Composition: 69.2-28.3-2.5 mol%)	Eutectic: 611 K (HMR~735 K) (Composition: 42.5-17-40.5 mol%) Peritectic: 705 K (Composition: 49.0-21.5-29.5 mol%)	Lower melting point and higher Peritectic/Eutectic gradient
	Vapour pressure/Boiling point (K) Figure 3	0.07 Pa at 1000 K Lowest vapour pressure/Highest boiling point	88.0 Pa at 1000 K High vapour pressure/Low boiling point	122.4 Pa at 1000 K Highest vapour pressure/Lowest boiling point
	Specific heat capacity (J/(mol·K)) Figure 4	~87.9 at melting point Lowest heat capacity	~494.9 at melting point Higher heat capacity	~579.0 at melting point Highest heat capacity
	Thermal conductivity (Watt/(m·K)) Equation (4)	~0.9078 constant Higher Thermal Conductivity	~0.3163 constant Lower Thermal Conductivity	~0.2611 constant Lowest Thermal Conductivity
	Density (gr/cm ³) Figure 5	$5.1720 - 0.9223 \times 10^{-3} T^*$ Highest Density vs. temperature	$4.1224 - 1.0117 \times 10^{-3} T$ Lowest Density vs. temperature	$5.1487 - 1.4316 \times 10^{-3} T$ Lower Density vs. temperature
	Neutronic design	Criticality Volume (cm ³) Table 9	1.39 Smallest critical size	2.54 Largest critical size
Neutron flux-energy spectrum Figure 9 and Table 10		Softer neutron flux-energy spectrum	Hardest neutron flux-energy spectrum	Hard neutron flux-energy spectrum

* T = temperature in kelvin.

Author Contributions: Conceptualization, B.M.; Data curation, O.N.-k. and B.M.; Formal analysis, O.N.-k.; Investigation, O.N.-k., G.C.-G. and B.M.; Methodology, O.N.-k. and B.M.; Resources, O.N.-k., D.L., A.D. and L.J.; Software, O.N.-k.; Supervision, O.N.-k. and B.M.; Validation, O.N.-k., D.L., A.D. and L.J.; Visualization, O.N.-k.; Writing—original draft, O.N.-k.; Writing—review and editing, O.N.-k., G.C.-G. and B.M. All authors have read and agreed to the published version of the manuscript.

Funding: The authors would like to extend their appreciation for the generous support of the Engineering and Physical Sciences Research Councils, EPSRC-UK (grant numbers: EP/V027239/1).

Data Availability Statement: The data can be shared up on request.

Conflicts of Interest: The authors declare no conflict of interest.

References

1. Pioro, I.L. Introduction: Generation IV International Forum. In *Handbook of Generation IV Nuclear Reactors*; Elsevier Ltd.: Amsterdam, The Netherlands, 2016. [CrossRef]
2. Merk, B.; Litskevich, D.; Peakman, A.; Benkhad, M. IMAGINE—A Disruptive Change to Nuclear or How Can We Make More Out of the Existing Spent Nuclear Fuel and What Has to be Done to Make it Possible in the UK? *Awt-Int. Z. Fuer Kernenerg.* **2019**, *64*, 353–359.
3. Merk, B.; Litskevich, D.; Whittle, K.R.; Bankhead, M.; Taylor, R.J.; Mathers, D. On a long term strategy for the success of nuclear power. *Energies* **2017**, *10*, 867. [CrossRef]
4. IAEA-TECDOC-1696; Challenges Related to the Use of Liquid Metal and Molten Salt Coolants in Advanced Reactors. International Atomic Energy Agency: Vienna, Austria, 2013.
5. Haubenreich, P.N.; Engel, J.R. Experience With the Molten-Salt Reactor Experiment. *Nucl. Appl. Technol.* **1970**, *8*, 118–136. [CrossRef]
6. Fratoni, M.; Shen, D.; Ilas, G.; Powers, J. Molten Salt Reactor Experiment Benchmark Evaluation. *Miskolc Math. Notes* **2020**, *21*, 51–60.
7. Prince, B.E.; Ball, S.J.; Engel, J.R.; Haubenreich, P.N.; Kerlin, T.W. *Zero-Power Experiments on the Molten-Salt Reactor Experiment*; Oak Ridge National Laboratory: Oak Ridge, TN, USA, 1968.
8. Thoma, R. *Phase Diagram of Nuclear Reactor Materials*; Oak Ridge National Laboratory: Oak Ridge, TN, USA, 1959.
9. US Atomic Energy Commission. *An Evaluation of the Molten Salt Breeder Reactor*; U.S. Government Printing Office: Washington, DC, USA, 1972.
10. Smith, J.; Simmons, W.E. *An Assessment of a 2500 MWe Molten Chloride Salt Fast Reactor*; Atomic Energy Establishment: Winfrith, UK, 1974.
11. EVOL (Project n°249696) Final Report. 2015. Available online: <https://cordis.europa.eu/project/id/249696> (accessed on 10 June 2022).
12. Final Report Summary—EVOL, CORDIS | European Commission [WWW Document]. 2013. Available online: <https://cordis.europa.eu/project/id/249696/reporting> (accessed on 30 June 2022).
13. Ignatiev, V.; Feynberg, O.; Gnidoi, I.; Konakov, S.; Kormilitsyn, M.; Merzliakov, A.; Surenkov, A.; Uglov, V.; Zagnitko, A. *MARS: Story on Molten Salt Actinide Recycler and Transmuter Development by Rosatom in Co-operation with Euratom*; Nuclear Energy Agency of the OECD (NEA): Paris, France, 2015.
14. Ignatiev, V.; Feynberg, O.; Gnidoi, I.; Merzlyakov, A.; Surenkov, A.; Uglov, V.; Zagnitko, A.; Subbotin, V.; Sannikov, I.; Toropov, A.; et al. Molten salt actinide recycler and transforming system without and with Th-U support: Fuel cycle flexibility and key material properties. *Ann. Nucl. Energy* **2014**, *64*, 408–420. [CrossRef]
15. A Paradigm Shift in Reactor Safety with the Molten Salt Fast Reactor [WWW Document]. CORDIS EU Research Results. 2019. Available online: <https://cordis.europa.eu/project/id/661891> (accessed on 10 June 2022).
16. Faure, B.; Kooyman, T. A comparison of actinide halides for use in molten salt reactor fuels. *Prog. Nucl. Energy* **2022**, *144*, 104082. [CrossRef]
17. Gakhar, R.; Phillips, W.C.; Cao, G.; Yoo, T.S.; Woods, M.E.; Fredrickson, G.L.; Karlsson, T. Molten Salt Fuels: Properties, Purification, and Corrosion Control. *Encycl. Nucl. Energy* **2021**, 366–376. [CrossRef]
18. Merk, B.; Litskevich, D.; Bankhead, M.; Taylor, R.J. An innovative way of thinking nuclear waste management—Neutron physics of a reactor directly operating on SNF. *PLoS ONE* **2017**, *12*, e0180703. [CrossRef]
19. Merk, B.; Litskevich, D.; Gregg, R.; Mount, A.R. Demand driven salt clean-up in a molten salt fast reactor—Defining a priority list. *PLoS ONE* **2018**, *13*, e0192020. [CrossRef]
20. Merk, B.; Detkina, A.; Atkinson, S.; Litskevich, D.; Cartland-Glover, G. Evaluation of the breeding performance of a NaCl-UCl₃-Based reactor system. *Energies* **2019**, *12*, 3853. [CrossRef]
21. Merk, B.; Detkina, A.; Litskevich, D.; Atkinson, S.; Cartland-Glover, G. The interplay between breeding and thermal feedback in a molten chlorine fast reactor. *Energies* **2020**, *13*, 1609. [CrossRef]
22. Merk, B.; Detkina, A.; Atkinson, S.; Litskevich, D.; Cartland-Glover, G. Evaluating reactivity control options for a chloride salt-based molten salt zero-power reactor. *Appl. Sci.* **2021**, *11*, 7447. [CrossRef]
23. Merk, B.; Detkina, A.; Atkinson, S.; Litskevich, D.; Cartland-Glover, G. On the dimensions required for a molten salt zero power reactor operating on chloride salts. *Appl. Sci.* **2021**, *11*, 6673. [CrossRef]
24. Merk, B.; Detkina, A.; Litskevich, D.; Drurdy, M.; Noori-Kalkhoran, O.; Cartland-Glover, G.; Petit, L.; Rolfo, S.; Elliot, J.P.; Mount, A.R. Defining the Challenges—Identifying the Key Poisoning Elements to Be Separated in a Future Integrated Molten Salt Fast Reactor Clean-Up System for iMAGINE. *Appl. Sci.* **2022**, *12*, 4124. [CrossRef]
25. Pelowitz, D.B. *Mcnp User' S Manual—Version 2.7.0*; Los Alamos National Laboratory: Los Alamos, NM, USA, 2011.

26. Chadwick, M.B.; Herman, M.; Obložinský, P.; Dunn, M.; Danon, Y.; Kahler, A.; Smith, D.; Pritychenko, B.; Arbanas, G.; Arcilla, R.; et al. ENDF/B-VII.1 nuclear data for science and technology: Cross sections, covariances, fission product yields and decay data. *Nucl. Data Sheets* **2011**, *112*, 2887–2996. [[CrossRef](#)]
27. Katyshev, S.; Teslyuk, L. Ionic Melts in Nuclear Power. In *Challenges and Solutions in the Russian Energy Sector*; Springer: Berlin/Heidelberg, Germany, 2018; pp. 181–189.
28. Capelli, E.; Beneš, O.; Colle, J.Y.; Konings, R.J.M. Determination of the thermodynamic activities of LiF and ThF₄ in the Li₂Th_{1-x}F_{4-3x} liquid solution by Knudsen effusion mass spectrometry. *Phys. Chem. Chem. Phys.* **2015**, *17*, 30110–30118. [[CrossRef](#)]
29. Baehr, H.D. Thermochemical properties of inorganic substances. *Forsch. Im Ing.* **1992**, *58*, 103. [[CrossRef](#)]
30. Bradley, D. *The Preparation and Properties of the Chlorides of Uranium, Plutonium, Thorium and of the Fission Product Chlorides*; A.E.R.E. Harwell Rep. OE/b 2215; Atomic Energy Research Establishment: Harwell, UK, 1957.
31. Ewing, C.T.; Stern, K.H. Equilibrium Vaporization Rates. *J. Phys. Chem.* **1974**, *78*, 1998–2005. [[CrossRef](#)]
32. Fiock, E.F.; Rodebush, W.H. The vapor pressures and thermal properties of potassium and some alkali halides. *J. Am. Chem. Soc.* **1926**, *48*, 2522–2528. [[CrossRef](#)]
33. Myers, P.D.; Goswami, D.Y. Thermal energy storage using chloride salts and their eutectics. *Appl. Therm. Eng.* **2016**, *109*, 889–900. [[CrossRef](#)]
34. Parker, S.S.; Long, A.; Lhermitte, C.; Vogel, S.; Monreal, M.; Jackson, J.M. Thermophysical properties of liquid chlorides from 600 to 1600 K: Melt point, enthalpy of fusion, and volumetric expansion. *J. Mol. Liq.* **2022**, *346*, 118147. [[CrossRef](#)]
35. Price, J.C.; Mariani, R.D. *Synthesis of Uranium Trichloride for the Pyrometallurgical Processing of Used Nuclear Fuel*; INL/CON-10-20111; Idaho National Lab: Idaho Falls, ID, USA, 2011.
36. Williams, D.F.; Toth, L.M.; Clarno, K.T. *Assessment of Candidate Molten Salt Coolants for the Advanced High-Temperature Reactor (AHTR)*; Ornl/Tm-2006/69; National Technical Information Service: Springfield, VA, USA, 2006.
37. Kopp, H. *Investigation of the Specific Heat of Solid Boses*; Royal Society: London, UK, 1864.
38. Leitner, J.; Voňka, P.; Sedmidubský, D.; Svoboda, P. Application of Neumann-Kopp rule for the estimation of heat capacity of mixed oxides. *Thermochim. Acta* **2010**, *497*, 7–13. [[CrossRef](#)]
39. Touloukian, Y.; Powell, R.; Ho, C.; Klemens, P. Thermal Conductivity-Nonmetallic Solids. 1971. Available online: <https://www.piping-designer.com/index.php/properties/878-tables/2728-thermal-conductivity-of-non-metallic-solids> (accessed on 5 July 2022).
40. Capelli, E.; Konings, R.J.M. Halides of the Actinides and Fission Products Relevant for Molten Salt Reactors. In *Comprehensive Nuclear Materials*, 2nd ed.; Elsevier Ltd.: Amsterdam, The Netherlands, 2020. [[CrossRef](#)]
41. Morss, L.R.; Edelstein, N.; Fuger, J.; Katz, J.J. *Chemistry of Actinide and Transactinide Elements*, 4th ed.; Springer: Berlin/Heidelberg, Germany, 2010.
42. Haupin, W. Hot wire method for rapid determination of thermal conductivity. *Am. Ceram. Soc. Bull.* **1960**, *39*, 139–141.
43. Cornwell, K. The thermal conductivity of molten salts. *Appl. Phys.* **1970**, *4*, 441–445. [[CrossRef](#)]
44. Gheribi, A.E.; Torres, J.A.; Chartrand, P. Recommended values for the thermal conductivity of molten salts between the melting and boiling points. *Sol. Energy Mater. Sol. Cells* **2014**, *126*, 11–25. [[CrossRef](#)]
45. Ignatiev, V.; Merzlyakov, A. Transport Properties of Molten-Salt Reactor Fuel Mixtures: The Case Of Na, Li, Be/F And Li, Be, Th/F Salts. In *Actinide and Fission Product Partitioning and Transmutation*; Nuclear Energy Agency of the OECD (NEA): Paris, France, 2003; pp. 581–590.
46. Rama Rao, M. Thermal Conductivity of Liquids. *Phys. Rev.* **1940**, *59*, 212.
47. Grimes, W.R. *Reactor Chemistry Division, Annual Progress Report for Period Ending December 31, 1965*; Oak Ridge National Laboratory: Oak Ridge, TN, USA, 1965. [[CrossRef](#)]
48. Grimes, W.R. *Annual Progress Report for Period Ending January 31, 1962*; Oak Ridge National Laboratory: Oak Ridge, TN, USA, 1962.
49. Desyatnik, V.; Katyshev, S. Volumetric and surface properties of the NaCl-UCl₃-UCl₄ melts. *Zhurnal Fiz. Khimii* **1980**, *54*, 1606–1610.